DE GRUYTER OPEN

ARCHIVES OF MECHANICAL TECHNOLOGY AND MATERIALS
WWW.AMTM.PUT.POZNAN.PL

Diagnosis of edge condition based on force measurement during milling of composites

Agata Felusiak [a]*, Paweł Twardowski [a]

[a] *Poznań University of Technology, Piotrowo 3, Poznań 61-138, Poland*

[*] *Corresponding author, Tel +48 690 035 682, e-mail address: felusiak.agata@gmail.com*

ARTICLE INFO

Received 19 September 2017
Received in revised form 05 February 2018
Accepted 03 April 2018

KEY WORDS

Neural network,
Metal Matrix Composite,
Cutting force,
Tool wear

ABSTRACT

The present paper presents comparative results of the forecasting of a cutting tool wear with the application of different methods of diagnostic deduction based on the measurement of cutting force components. The research was carried out during the milling of the Duralcan F3S.10S aluminum-ceramic composite. Prediction of the tool wear was based on one variable, two variables regression, Multilayer Perceptron (MLP) and Radial Basis Function (RBF) neural networks. Forecasting the condition of the cutting tool on the basis of cutting forces has yielded very satisfactory results.

1. INTODUCTION

At the turn of recent years we can see more and more new materials on the market, which cutting properties are not fully known. The development of the automotive industry, aviation, etc. makes new and more durable materials needed, and the components made as accurate as possible in the shortest possible time. Metal-ceramic composites have found their use in recent applications because of better properties than light metals without additives or pure ceramics. They exhibit increased tensile and flexural strength, greater thermal expansion, greater tolerance to damage, and better tribological properties [5]. Metal-ceramic composites are multiphase materials consisting of metal and ceramics and may have other phases, but the volumetric fraction of the metallic phase must be more than a half of the composition of the material. These materials are mainly manufactured to modify mechanical properties (increase in hardness and stiffness), wear resistance due to friction, creep reduction. These composites have been used inter alia for aircraft chassis components, brakes, engine and turbine parts [7]. Metal-ceramic composites are difficult to cut and require the supervision of the cutting process.

The essence of monitoring the milling process is the ability to predict a tool wear, workpiece quality, enabling full automation of the cutting process by determining the condition of the used tool. Without cutting monitoring systems, it is not possible to eliminate the costs associated with too early tool replacement. Tool wear is a random occurrence because of a large number of factors affecting to them [4]. Using the diagnostic tools for cutting tool and process allows higher cutting parameters to be used, making it possible to exploit the potential capabilities of the machining system entirely [3]. Determining the right time to replace the tool, so the tool reaches the limit of wear is one of the most important tasks of diagnostic systems. The edge wear occurs at significantly less time than the wear of the other parts of the system, such as spindle or tool holder. Generally, it can be stated that diagnosis of the cutting process is to ensure the quality of the product while minimizing the wear costs of the machining system components. The components of cutting, vibration and acoustic emissions are usually used to the supervision.

DOI: 10.2478/amtm-2018-0002

Whereof the signals of the cutting force components, and in particular the resistance force, are most resistant to interference from the kinematic systems of the machine [2].

Diagnostic implication is understood as the processing of a diagnostic test result and other information about a subject and its environment, which is the final step in the diagnosis process and results in a diagnosis. During diagnostic inference a useful tool is neural networks. The neural networks are helpful in determining the relationships between data, while using them, it is possible to find a dependency model without prior assumptions about it. Multilayer unidirectional networks (MLPs), are most commonly used, this means that the network only provides forward information (from input to output), there is no feedback here, this network has been used in this paper. Such a network consists of one input layer, hidden n-layers (usually one or two) and one output layer. Information on this network is transmitted on a peer-to-peer basis (P2P) [3,9]. Another type of network, also used in this paper, is a network with radial basis functions (RBF). In these networks, the output values of neurons depend on the distance of the test point from the center, and the center is expressed by the learning parameters of the radial neuron. Important indicators of correctness during the working network analysis are the quality of learning, validation and testing indicators. These values are correlation coefficients, which are the mean of all data in the validation and test learning sets. The error value that is usually calculated as a mean squared error is also important [1,10].

2. OBJECTIVE, SCOPE AND EXPERIMENTAL PROCEDURES

2.1. Scope of research

The purpose of the work is to demonstrate the suitability of cutting forces in diagnosing the condition of the edge during milling of hard-wear materials such as aluminum-ceramic composites and compare to the most common diagnostic methods.

As a workpiece, an aluminum-ceramic (Al-SiC) – Duralcan. Alloy F3S.10S. was used. The chemical composition of the composite is shown in Table 1 [11].

Table 1.Chemical composition of aluminum-ceramic composite F3S.10S

Si %	Fe %	Cu %	Mg %
8,50-9,50	to 0,20	to 0,20	0,45-0,65
Ti %	SiC %	others %	Al
to 0,20	to 10	to 0,03 together 0,01	rest

This alloy is gravity casting and designed for rotors of railway brakes, brake calipers, cylinder liners and laser sensor housings. It is characterized by high thermal stability and low abrasive wear and low thermal stress [11]. Figure 1 shows the metallographic sample of the ingot used in the test.

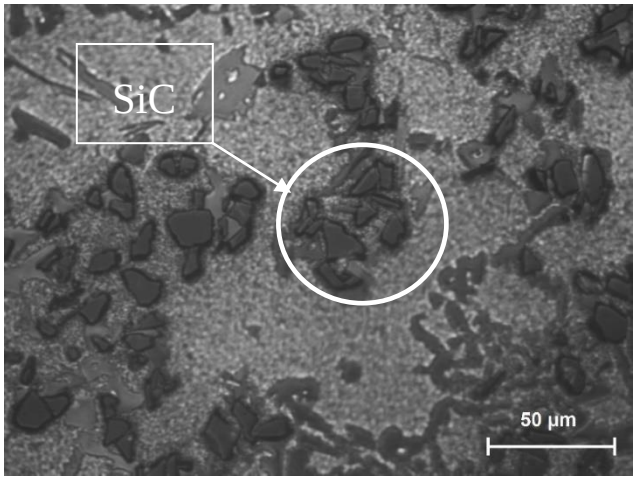

Fig. 1. **Metallographic sample of F3S.10S**

The machining was done on a universal milling machine with the following parameters:
- f_z = 0.02 mm / rev
- f_t = 84 mm / tooth
- n = 1400 rpm
- a_p = 5 mm
- a_e = 0.5 mm
- L = 278 mm

Six monolithic, 3-fluted, milling cutters made by Kennametal with a diameter of Ø 10 mm, made of cemented carbide K600, were used during the machining. This cutter is designed for milling aluminum alloys.

2.2. *Method of measurement*

With a triaxial piezoelectric force gauge, the force values were measured during the milling of the Duralcan ingot. The principle of operation of the gauge is based on three piezoelectric sandwich transducers, which are preloaded to allow transfer forces tangential to the surface of the plates. The *Fc* component force is measured by the pair of plates cut perpendicular to the electric axis x of the crystal. The feed and thrust components are measured with two pairs of plates cut perpendicular to the mechanical axis y of the crystal. The electric axes of both plates relative to each other are rotated 90° [12].

During the research, six Kennametal monolithic, 3-point milling cutters, Ø 10mm in diameter, made of sintered carbides with the designation K600 were used. During each pass, the cutting forces were measured, and after each pass the VBB consumption value was measured. The data from the five cutters was used as input data, with the consumption value being the average of the wear on each cutter surface. The data collected during the last milling (tool 5) were used for tests of designated functions and neural networks. The test results were shown in Table 2.

Figure 2 shows a diagram of the measuring path for measuring the forces during milling. A three-piece piezoelectric vibration sensor collects information about the force component values. Then the signal is transmitted to the amplifiers and the upper and lower pass filters, after which the amplified signal is converted to a digital signal and sent to the computer with the corresponding program for recording and analysis.

Table 2. Peak and mean values of force components in time and wear values after each pass

tool	T [min]	VB_B [mm]	F_{pmax} [N]	F_{fmax} [N]	F_{fNmax} [N]	F_{prms} [N]	F_{frms} [N]	F_{fNrms} [N]
1	3,31	0	241	257	211	100	92	75
	6,62	0	187	224	180	77	78	55
	9,93	0	207	209	223	86	79	75
	13,24	0	215	221	153	97	85	51
	16,55	0,07	208	198	174	85	75	62
	19,86	0,07	181	197	171	71	70	59
	23,17	0,08	248	228	310	91	90	120
	26,48	0,14	283	334	454	110	131	186
	29,79	0,2	320	382	552	109	122	237
	33,1	0,3	310	365	618	125	143	255
	36,41	0,31	310	386	699	130	161	285
2	3,31	0,19	241	257	435	118	121	202
	6,62	0,22	273	303	547	120	137	252
	9,93	0,25	320	301	690	137	148	305
	13,24	0,29	316	444	738	135	172	308
	16,55	0,33	348	485	796	148	175	348
3	3,31	0,13	230	274	426	102	118	186
	6,62	0,21	311	350	501	124	151	219
	9,93	0,25	298	332	648	128	152	268
	13,24	0,3	331	472	606	126	176	269
	16,55	0,35	366	469	694	132	145	301
4	3,31	0,18	313	405	455	109	132	200
	6,62	0,21	316	399	577	131	163	256
	9,93	0,25	357	363	659	151	161	301
	13,24	0,28	454	366	696	129	155	303
	16,55	0,33	239	428	772	78	162	369
	19,86	0,38	220	524	796	73	170	370
5	3,31	0,18	159	325	451	45	93	212
	6,62	0,22	221	359	604	68	119	283
	9,93	0,26	194	463	657	58	139	316
	13,24	0,3	201	470	753	65	156	348
	16,55	0,36	193	512	870	62	164	371
	19,86	0,41	211	461	880	68	157	401
6	3,31	0,21	181	334	488	73	97	237
	6,62	0,24	216	406	682	68	129	324
	9,93	0,28	230	380	665	64	129	330
	13,24	0,32	217	389	787	69	133	380
	16,55	0,39	194	447	807	65	137	382
	19,86	0,45	199	501	730	69	158	389

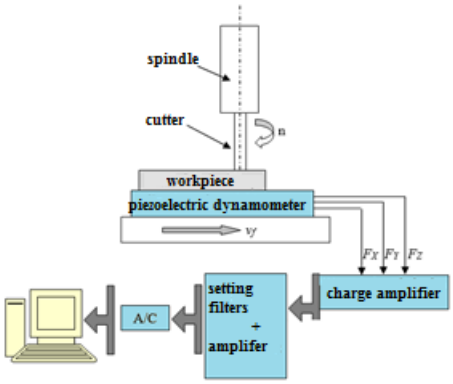

Fig. 2. Diagram of measurement circuit

Figure 3 shows how to mount the dynamometer and the axis and force components.

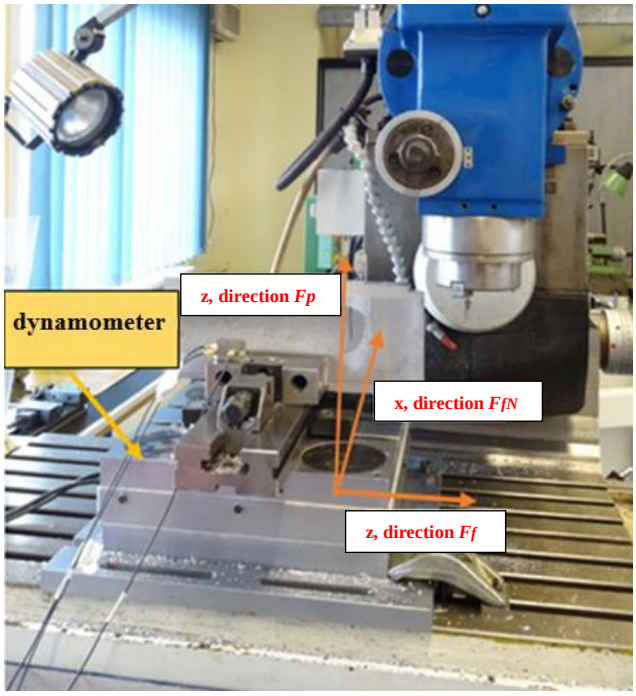

Fig. 3. Mounting position of the dynamometer and axle markings

After each pass, the wear of each tool wear (VB_B) was measured using a PZO MWM 2373 workshop microscope. The analysis yields two values for each force component, the mean square and the maximum. Both values were calculated from the final run of each pass to match the final wear values. The mean square value is calculated according to formula 1.

$$\psi_x = \sqrt{\lim_{T\to\infty}\frac{1}{T}\int_0^T x^2(t)dt} \tag{1}$$

The peak is the maximum amplitude value for a certain period of time.

3. TEST RESULTS AND ANALYSIS

Total edge wear usually took five passes i.e. a cutting time of approx. t=17 min. With a limitation value VB_B=0.3 mm. A measure scheme of the VBB wear on milling tool are shown in Figure 4. Figure 5. shows a comparison between a new tool and a damaged tool.

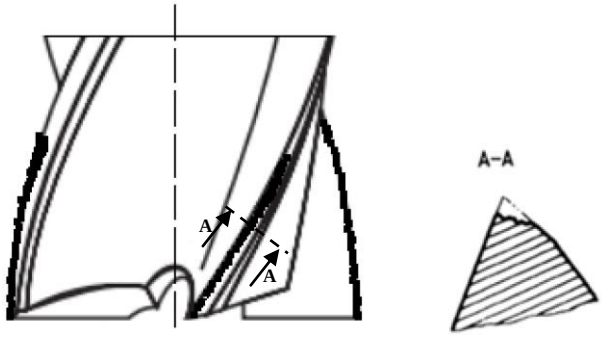

Fig. 4. Wear flank face (VB_B)

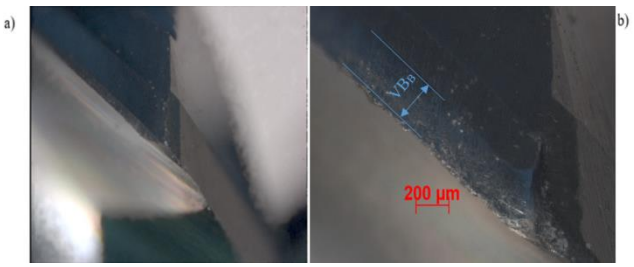

Fig. 5. a) New tool, b) wear flank face on milling tool

3.1. Analysis of force waveform signals in the time domain

Based on the data recorded in *Analizator* program, the waveform components of the cutting forces signals in the time domain were obtained. Sample waveforms are shown in Figure 5.

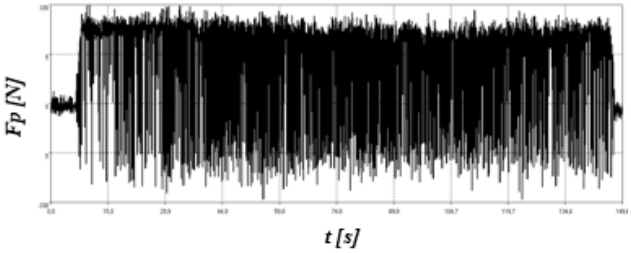

Fig. 5. The waveform of the Fp component in the time domain

Based on the obtained graphs, the peak and the mean square component forces of the time domain were calculated.

3.2. Spectral analysis of component cutting forces

Using the *Analizator* program, the waveform components of the cutting forces signals in the frequency domain were obtained. Conversion from time-domain to frequency-based signal is based on Fast Fourier Transform (FFT). As it is seen in Figure 6, the dominant spectrum component is for frequency f=69Hz. As shown by the formula 2, this is the frequency resulting from the insertion of the cutting edge into the material.

$$f_{input} = \frac{n \cdot z}{60} = \frac{1400 \cdot 3}{60} = 69[Hz] \qquad (2)$$

4. *DIAGNOSTIC INFERENCE BASED ON REGRESSION OF ONE VARIABLE*

From the set of values of the machining forces of the time and frequency domain, the linear correlation of the data is equal to or higher than $R^2 \geq 0{,}7$, because according to the literature data [6,13], such a coefficient provides a strong linear correlation of the data. Based on trendline formulas predicted tool wear values were received and square root of mean square error values were computed after comparison with the data of reference milling (cutter 5). Figures 7, 8 show exemplary graphs based on time progres. As a result of the increasing flank face wear, the cutting force increases [8], this is related to the increase of cutting resistance. So an increase in the value of the cutting force components signal allows to conclude about the increase in wear. This dependence is presented in graphs 7,8 and regression function models in Table 2 . The lowest error value was obtained for the maximum values and the mean square of normal force, which is consistent with the literature data. In the frequency domain, from the diagnostic point of view, only the normal component for the first tool frequency of input in the material (f_{input}) is useful. In no case has the correlation between the component of F_p and the wear of the VB_B edge been observed. Table 3. presents predicted wear, mean square errors calculated on the basis of equations from Table 2.

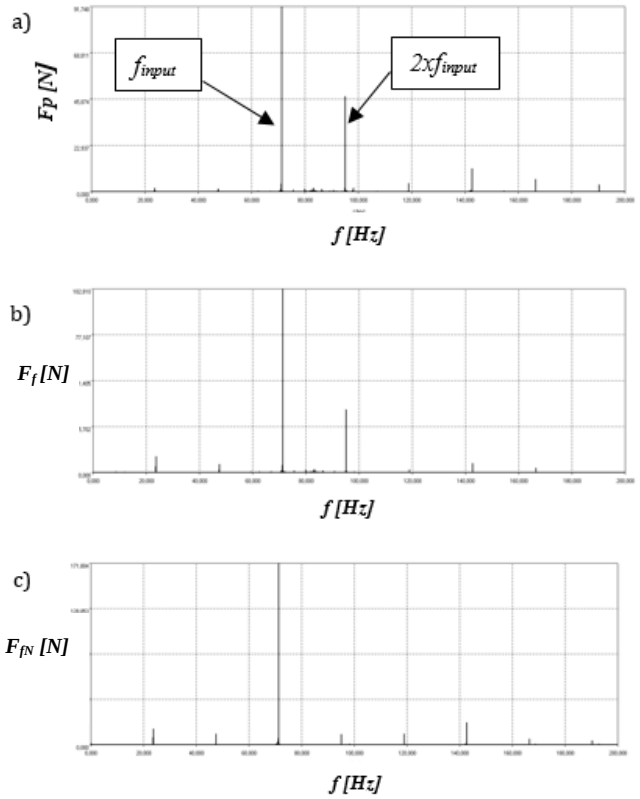

Fig. 6. Waveform spectrum of force components; a) component according to direction of cutting speed F_p; b) component of feed F_f, c) normal component F_{fN}

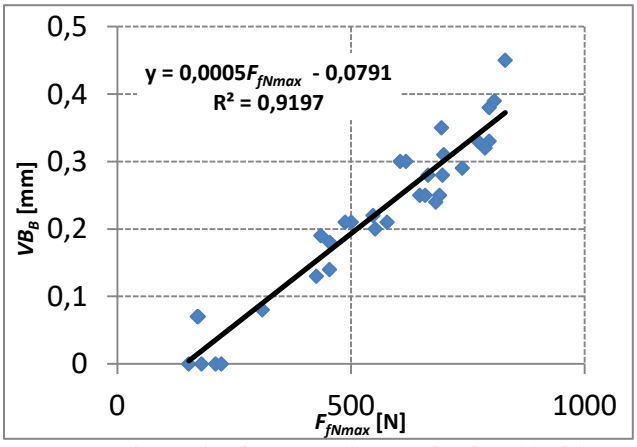

Fig. 7. Dependency of tool wear VB_B from peak value of feed force

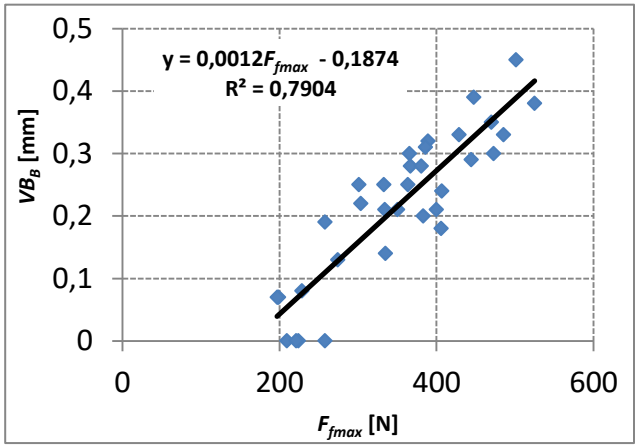

Fig. 8. Dependency of tool wear VB_B from peak value of normal force

Table 2. Linear regression functions of one variable

nr	variable	wear equation
1.	F_{fNmax}	$VB_B=0{,}0012 \cdot F_{fNmax}-0{,}790$
2.	F_{fNmax}	$VB_B=0{,}0005 \cdot F_{fNmax}-0{,}079$
3.	F_{fRMS}	$VB_B=0{,}0032 \cdot F_{fRMS}-0{,}198$
4.	F_{fNRMS}	$VB_B=0{,}0011 \cdot F_{fNRMS}-0{,}046$
5.	$F_{fNinput}$	$VB_B=0{,}0005 \cdot F_{fNinput}-0{,}0791$

Table 3. Expected tool wear values and the mean square root error and linear regression functions

real	theoretical				
VB_B for cutter 5 [mm]	VB_B for F_{fmax} [mm]	VB_B for F_{fNmax} [mm]	VB_B for F_{fRMS} [mm]	VB_B for F_{fNRMS} [mm]	VB_B for $F_{fNinput}$ [mm]
0,18	0,2027	0,1465	0,1005	0,1879	0,1888
0,22	0,2442	0,2233	0,1846	0,2661	0,2622
0,26	0,3687	0,2496	0,2464	0,3028	0,2836
0,3	0,3773	0,2975	0,3024	0,3379	0,3414
0,36	0,4278	0,356	0,3290	0,3628	0,3385
0,41	0,3660	0,3611	0,3066	0,3961	0,3576
error	0,0651	0,0247	0,0569	0,0307	0,0350

5. DIAGNOSTIC IMPLICATIONS BASED ON REGRESSION OF TWO VARIABLES

Using *Statistica*, three-dimensional graphs of tool wear VB_B vs two components of force were created. Fig. 9. illustrates an exemplary graph depicting the dependence of wear of the component forces. The dependencies in which the square root of mean square error was the smallest, i.e. the predicted values of wear on the basis of the quadratic formula describing the surfaces of the graph, are closest to the values obtained in the reference pass (cutter 5).

Table 4. presents the mathematical functions of the various planes describing the relationship between the force components and the wear of the edge VB_B. Table 5. shows the predicted results of wear, the values of square root of mean square errors.

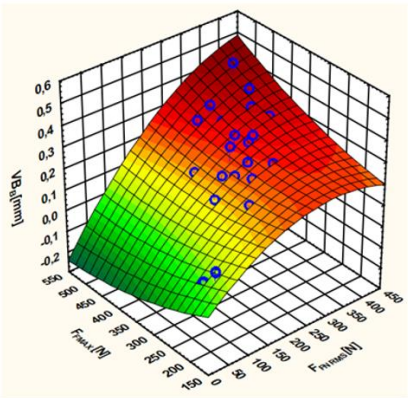

$$VBB = 0{,}14+0{,}0013 \cdot F_{fNrmS}-0{,}0013 \cdot F_{fmax}-2{,}71 \cdot 10^{-6} \cdot F_{fNrms} \cdot F_{fNrms}+2{,}81 \cdot 10^{-6} \cdot F_{fNrms} \cdot F_{fmax}+1{,}08 \cdot 10^{-6} \cdot F_{fmax} \cdot F_{fmax}$$

Fig.9. Dependency of wear VB_B from F_{fmax} and F_{fNRMS}

Table 4. Functions showing the dependence between cutting force components and wear VB_B

V_{BB} for F_{fmax},F_{fNRMS} [mm]	V_{BB} for F_{fNmax}, F_{fRMS} [mm]	V_{BB} for F_{fmax}, F_{fNmax} [mm]	V_{BB} for F_{fNRMS},F_{fRMS} [mm]
$VB_B=0{,}14+0{,}0013 \cdot F_{fNRMS}-0{,}0013F_{fmax}-2{,}71 \cdot 10^{-6} \cdot F_{fNRMS}^2+2{,}81 \cdot 10^{-6} \cdot F_{fNRSM} \cdot F_{fmax}+1{,}08 \cdot 10^{-6} \cdot F_{fmax}^2$	$VB_B=0{,}075-0{,}0032 \cdot F_{fRMS}-0{,}0007 \cdot F_{fNmax}+1{,}4 \cdot 10^{-5} \cdot F_{fRMS}^2-9{,}51 \cdot 10^{-7} \cdot F_{fRMS} \cdot F_{fNmax}-3{,}03 \cdot 10^{-8} F_{fNmax}^2$	$VB_B=0{,}16+0{,}009 \cdot F_{fNmax}-0{,}002 \cdot F_{fmax}-4{,}06 \cdot 10^{-7} \cdot F_{fNmax}^2+9{,}99 \cdot 10^{-8} \cdot F_{fNmax} \cdot F_{fmax}+2{,}91 \cdot 10^{-6} \cdot F_{fmax}^2$	$VB_B=0{,}086-0{,}0022 \cdot F_{fRMS}-0{,}001 \cdot F_{fNRMS}+5{,}34 \cdot 10^{-6} \cdot F_{fRMS}^2-4{,}46 \cdot 10^{-6} \cdot F_{fRMS} \cdot F_{fNRMS}-1{,}01 \cdot 10^{-6} F_{fNRMS}^2$

Table 5. Estimated consumption values based on regression of two variables

real	theoretical			
V_{BB} dla frezu 5 [mm]	V_{BB} for F_{fmax} ,F_{pRMS} [mm]	V_{BB} for F_{pmax}, F_{fRMS} [mm]	V_{BB} for F_{fmax}, F_{pmax} [mm]	V_{BB} for F_{pRMS},F_{fRMS} [mm]
0,18	0,183534	0,168446	0,153544	0,182982
0,22	0,253482	0,236789	0,23273	0,253609
0,26	0,326401	0,261914	0,303095	0,296093
0,3	0,356745	0,31637	0,344601	0,342788
0,36	0,406069	0,379136	0,418282	0,374645
0,41	0,379741	0,380632	0,373031	0,394357
error	0,0443	0,0179	0,0397	0,0281

6. DIAGNOSTIC INFERENCE BASED ON NEURAL NETWORKS

Two MLP and RBF network models were used in the work, networks were created that worked on different data sets. Table 6. shows the network formulas and variables for which the network was created. Where: MLP (RBF) 3-3-1 is an MLP (RBF) network type with three neurons in the input layer, three in the hidden layer and one in the output layer.
BFGS 42 - backward error propagation with 42 iterations
RBFT - RBF network teaching

Table 7 presents predicted tool wear and square roots of mean square errors.

Table 6. Selected neural networks and their properties

	name	quality of learning	quality testing	qualityof validation
1.	RBF 6-3-1	0,940292	0,995692	0,797116
2.	RBF 6-6-1	0,956241	0,983143	0,806295
3.	MLP 6-8-1	0,968468	0,975457	0,891897
4.	MLP 6-10-1	0,971616	0,978304	0,872292
5.	RBF 3-11-1	0,970593	0,917281	0,722665
6.	RBF 3-3-1	0,951669	0,970349	0,806752
7.	MLP 3-3-1	0,962926	0,962363	0,905039
8.	MLP 3-4-1	0,977273	0,964475	0,992969
9.	RBF 3-17-1	0,947367	0,986973	0,915829
10.	RBF 3-14-1	0,976525	0,999955	0,934198
11.	MLP 3-6-1	0,979250	0,972938	0,897118
12.	MLP 3-4-1	0,973250	0,976308	0,893461
	testing error	**learning algorithm**	**error function**	**activation hidden**
1.	0,001368	RBFT	SOS	Gauss
2.	0,000559	RBFT	SOS	Gauss
3.	0,000352	BFGS 62	SOS	Sinus
4.	0,000412	BFGS 33	SOS	Logistic
5.	0,000831	RBFT	SOS	Gauss
6.	0,000570	RBFT	SOS	Gauss
7.	0,000375	BFGS 41	SOS	Exponential
8.	0,000725	BFGS 58	SOS	Logistic
9.	0,000645	RBFT	SOS	Gauss
10.	0,000415	RBFT	SOS	Gauss
11.	0,000328	BFGS 62	SOS	Logistic
12.	0,000401	BFGS 44	SOS	Exponential
	learning error		**Validation error**	
1.	0,000787		0,001682	
2.	0,000582		0,001189	
3.	0,000425		0,001311	
4.	0,000435		0,001200	
5.	0,000394		0,002634	
6.	0,000641		0,001108	
7.	0,000495		0,001164	
8.	0,000306		0,001442	
9.	0,000715		0,001243	
10.	0,000317		0,000993	
11.	0,000279		0,001240	
12.	0,000359		0,001262	
	input activation		**data**	
1.	Linear		all F	
2.	Linear		all F	
3.	Logistic		all F	
4.	Logistic		all F	
5.	Linear		only F_{RMS}	
6.	Linear		only F_{RMS}	
7.	Logistic		only F_{RMS}	
8.	Sin		only F_{RMS}	
9.	Linear		only F_{MAX}	
10.	Linear		only F_{MAX}	
11.	Linear		only F_{MAX}	
12.	Exponential		only F_{MAX}	

Table 7. Predicted tool wears obtained using neural networks

VB_B for cutter 5 [mm]	RBF 6-3-1	RBF 6-6-1	MLP 6-8-1	MLP 6-10-1
0,18	0,169413	0,168609	0,119494	0,125082
0,22	0,204339	0,220483	0,237293	0,224657
0,26	0,291854	0,313287	0,291740	0,304288
0,3	0,339470	0,349836	0,327814	0,335287
0,36	0,393932	0,382849	0,352792	0,366209
0,41	0,380747	0,375456	0,358187	0,360368
error	**0,0287**	**0,0346**	**0,0376**	**0,0381**
VB_B for cutter 5 [mm]	RBF 3-11-1	RBF 3-3-1	MLP 3-3-1	MLP 3-4-1
0,18	0,219829	0,169234	0,131312	0,236957
0,22	0,250397	0,250033	0,233954	0,213042
0,26	0,307211	0,313769	0,279988	0,262360
0,3	0,341965	0,349240	0,335329	0,331406
0,36	0,357312	0,367953	0,357934	0,365242
0,41	0,362477	0,372790	0,369616	0,379507
error	**0,0382**	**0,0360**	**0,0312**	**0,0296**
VB_B for cutter 5 [mm]	RBF 3-17-1	RBF 3-14-1	MLP 3-6-1	MLP 3-4-1
0,18	0,205031	0,137877	0,165251	0,181655
0,22	0,203643	0,207059	0,255001	0,252082
0,26	0,298483	0,279469	0,304527	0,312147
0,3	0,356456	0,380369	0,347715	0,344329
0,36	0,412634	0,368161	0,404776	0,384225
0,41	0,352781	0,349409	0,374337	0,366328
error	**0,0440**	**0,0457**	**0,0387**	**0,0370**

Based on the above tables, it is clear that RBF networks interference is better only when the mean square are used at the same time with peak values. In other cases, better results are obtained using the MLP network.

7. COMPARISON OF INFERENCE METHODS

Table 8. summarizes the lowest error values for each of the inference methods. As it is seen in the table below, the smallest error value was obtained on the basis of two variables. However, the advantage of neural networks is the use of more variables so that the results are not so sensitive to accidental changes in one of the signals. Conclusion on the basis of only one variable implies the risk of interference and may therefore not be able to fulfill its task in on-line monitoring.

Table 8. Comparison of error values from all inference methods

name	network MLP 3-4-1	network RBF 6-3-1	regression of one variable	regression of two variables
date	F_{pRMS}, F_{cRMS}, F_{fRMS}	all	F_{pMAX}	F_{pmax}, F_{fRMS}
error	**0,0296**	**0,0287**	**0,0247**	**0,0179**

As can be seen in the table above, all of the presented inference methods allow to predict precisely the wear of a cutting tool (RMSE<0.03mm).

8. CONCLUSIONS AND SUMMARY

1. The studied material had a heterogeneous structure, which is visible on metallographic samples. This results in different wear intensity of the milling cutters. However, this had no significant effect on the predicted edge wear values.
2. Inference on the basis of the component force signals produces satisfactory results, and the predicted values are burdened with a small error. The normal component F_{fN} is most sensitive to milling tool wear, which means that tool wear has the greatest impact on its value. However, there was no satisfactory correlation between the wear of the tool and the cutting force Fp.
3. Using neural networks as a diagnostic inference method gives satisfactory results, but the results show that finding the best performing network architecture is not obvious. In order to resolve this, many different types of networks should be tested and this in turn is very time consuming. In addition, it is possible to use multiple variables of the cutting force, so that the interference of one signal does not have as significant consequences as in the case of the one-variable regression.
4. As can be seen from the presented studies, the diagnostic inference using cutting force components is more effective in the time domain than in the frequency domain. There is a greater correlation of the measures determined here from time passes.
5. The best results (smallest square root of mean square error RMSE=0.0179) were obtained for the regression of two variables F_{fNmax} and F_{fRMS}.

REFERENCES

[1] **Bullinaria J.,** Radial Basis Function Networks: Introduction, Neutral Computation: Lecture 13, 2015.

[2] **Burek J., Babiarz R., Sułowski P., Sałata M.,** Diagnostyka procesu wysokowydajnościowego frezowania stopów aluminium, Mechanik nr 11/2016, pp. 1652-1653.

[3] **Jemielniak K.**, Automatyczna diagnostyka stanu narzędzia i procesu skrawania, Oficyna Wydawnicza Politechniki Warszawskiej, Warszawa, 2002. pp. 3-8, 159-172.

[4] **Kumar R., Chattopadhyaya S., Hloch S., Krolczyk G., Legutko S.,** Wear characteristics and defects analysis of friction stir welded joint of aluminium alloy 6061-t6, Eksploatacja i niezawodność, Volume 18, Issue 1, 2016, Pages 128-135

[5] **Lenke I. Rogowski D.,** Design of metal ceramic composites, International Jurnal of Materials Research 95(5), pp. 676-680, 2006.

[6] **Mukaka M.,** A guide to appropriate use of Correlation coefficient in medical research, Malawia Medical Journal 24(3), pp. 69-71, 2012.

[7] **Surowska B., Śliwa R.,** Metaliczne materiały kopozytowe w aplikacjach lotniczych w tym materiały typu *GLARE,* III Konferrencja Roczna, 2010.

[8] **Thamizhmanii S., Hasan S.,** Relationship between flank wear and cutting force on the machining of hard martensitic stailess steel by super hard tools. Proceedings of the World Congress on Engineering 2010 Vol III WCE 2010, London, June 30 - July 2, 2010

[9] **Zhou D., Liu W., Zhou W., Dong S.,** Research on network traffic identification based on multi layer perceptron, Telkomnika (Telecommunication Computing Electronics and Control) 12(1), pp.201-208, 2014.

[10] http://www.rosczak.com/mlp/mlp.html (16.06.2017).

[11] https://www.rtapublicsales.riotinto.com/En/OurProducts/Documents/FicheDuralcan_Eng-rev%202016-04-19%20CROP.PDF (16.06.2017).

[12] http://layer.uci.agh.edu.pl/pl/dydaktyka/lab-sens/cw1.html (20.05.2017).

[13] http://home.agh.edu.pl/~bartus/index.php?action=dydaktyka&subaction=statystyka&item=regresja_i_korelacja (16.06.2017).